Bulletin of Earth Sciences of Thailand

Petrography and deformation history of the Three Pagodas Fault, western Thailand

Sittiporn Kongsukkho [1], Pitsanupong Kanjanapayont [1,2,*]

[1] *Basin Analysis and Structural Evolution Research Unit (BASE RU), Department of Geology, Faculty of Science, Chulalongkorn University, Bangkok 10330, Thailand*
[2] *M.Sc. Program in Petroleum Geoscience, Faculty of Science, Chulalongkorn University, Bangkok, 10330, Thailand*
** Corresponding author e-mail: pitsanupong.k@hotmail.com*

Received: 10 Nov 2021
Revised: 26 Dec 2021
Accepted: 28 Dec 2021

Abstract

The Three Pagodas Fault has formed as a result of the collision between the Indian plate and the Eurasia plate. The geology mainly consists of migmatitic gneiss, augen gneiss, marble, schist, quartzite, calc-silicate, metamorphosed under amphibolite to granulite facies. Field mapping and microstructure analysis were applied to reveal the kinematic history of the Three Pagodas Fault. The evolution of the strike-slip zone can be divided into D_1 and D_2. The early part of the first stage is D_{1a} involving ductile sinistral shearing and metamorphism. Foliations show the NW-SE striking with variably dipping between east to west, and the stretching lineations are well developed in NW-SE trending with sub-horizontal plunging to the south. This stage shows a NW-SE ductile deformation with a sinistral shearing. The subsequent D_{1b} is dominated by sinistral transpression related to the exhumation of a lens shape of this high-grade metamorphic complex. The last stage (D_2) is represented by dextral strike-slip fault, which is the inversion of this strike-slip system.

Keywords: Deformation, strike-slip fault, Three Pagodas Fault, Thailand

1. Introduction

The collision between the Indian and Eurasia plate influences the complex structures and tectonics in the Cenozoic (e.g., Tapponnier et al., 1982, 1986; Huchon et al., 1994; Lacassin et al., 1997; Morley, 2002). This continental collision took place at about 50-45 Ma ago (Molnar and Tapponnerier, 1975). It has resulted in the complex structure along Himalayas-Tibetan plateau and in the movement along the strike-slip faults both in the eastern Tibet and SE Asia (Chung et al., 1997, 1998, 2005; Lacassin et al., 1997; Lin et al., 2012). According to the model of the extrusion tectonics, the strike-slip faults in South China (e.g., the Jiale Fault, the Altyn Tagh Fault) and in SE Asia (e.g., Sagaing Fault in Myanmar, the Ailao Shan – Red River Fault in Yunnan and Vietnam, the Mae Ping Fault and the Three Pagodas Fault in Thailand) present the sinistral movement (Tapponnier et al., 1986; Leloup et al., 1995; Lacassin et al., 1997; Rhodes et al., 2005), which begin at 40-50 Ma (Lacassin et al., 1997, Upton, 1999, Nantasin et al., 2012, Simpson et al., 2021, Osterle et al., 2019, Palin et al., 2013, Kanjanapayont et al., 2013). Recently, focal mechanism solutions and regional geomorphology indicate reverse motion on these strike-slip faults (Tapponnier et al., 1986; Lacassin et al., 1997; Charusiri et al., 2002; Morley, 2002; Rhodes et al., 2005) in approximately between 30-37 Ma (Lacassin et al., 1997; Upton et al., 1997; Simpson et al., 2021; Morley et al., 2007). The explanation about the different motion possibly involves the changing of the stress field within this region (Huchon et al., 1994; Richter and Fuller, 1996).

The Three Pagodas Fault is characterized by a NW-SE trending (e.g., Bunopas, 1981, Kanjanapayont, 2015) (Fig. 1). The Three Pagodas Fault lies parallel southward to the Mae Ping shear zone (Tapponnier et al., 1986; Lacassin et al., 1997; Morley, 2002). The strike-slip models in SE Asia region suggested that the NW-SE systems, including the Three Pagodas Fault, were developed by sinistral movement in the early stage and were reactivated by dextral shearing in the later stage (e.g., Huchon et al., 1994; Lacassin et al., 1997; Rhodes et al., 2005). The mylonites in the Three Pagodas Fault have been subjected to high-grade metamorphic rock with sheared deformation (e.g., Nantasin et al., 2012; Kanjanapayont et al., 2018; Salypongse et al., 2020). The quartz mylonites in this shear zone indicated the 2-dimensional strain ratio (R_s) in XZ-plane of 1.60-1.97 with the simple shear component (Kanjanapayont et al., 2018). The later reactivation phase involved the developing development of a Tertiary pull-apart basin (Rhodes et al., 2005).

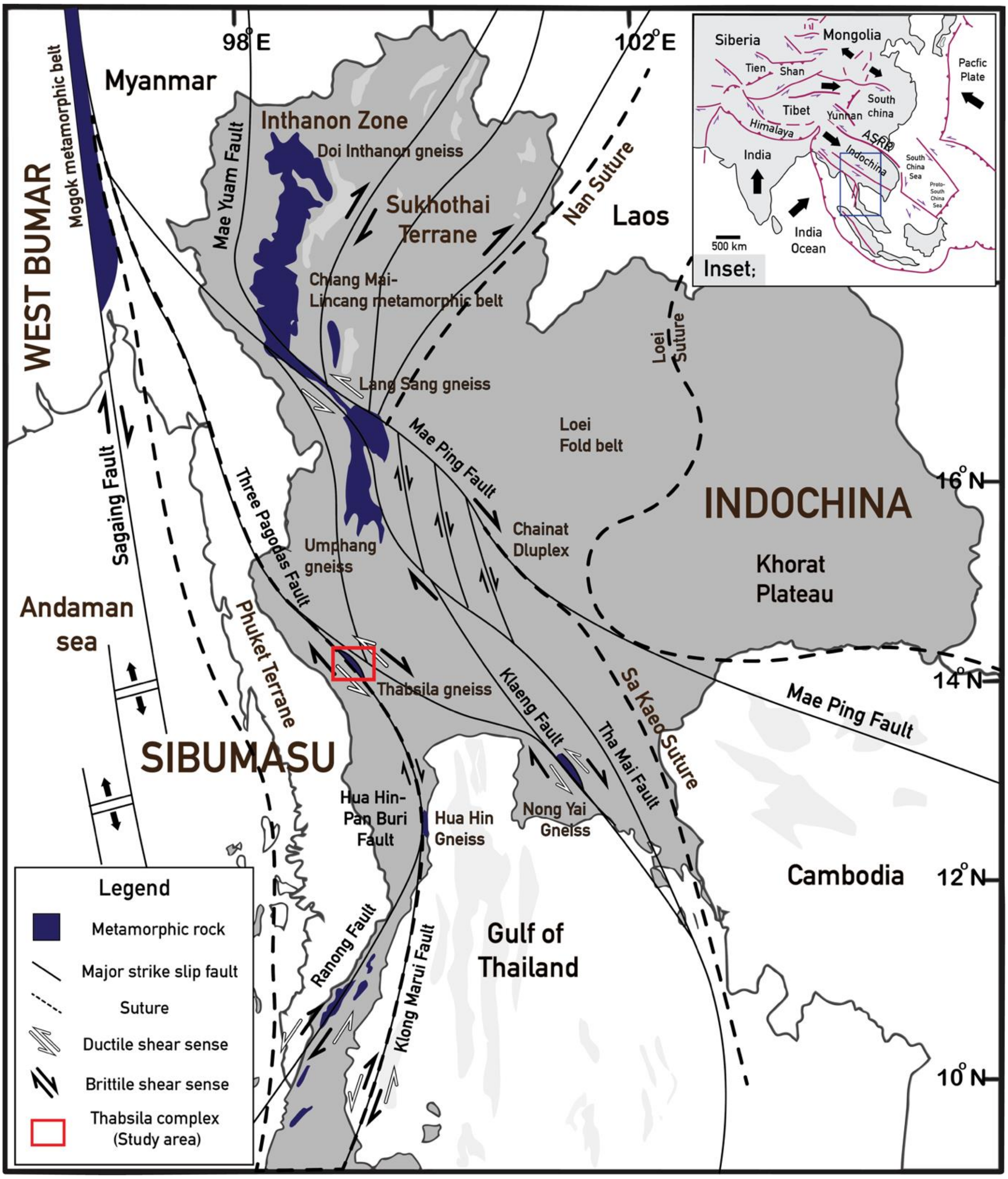

Figure 1 The major strike-slip faults in Thailand and the location of the Three Pagodas Fault (Modified from Tulyatid, 1991; Macdonald et al., 1993; Morley, 2002, 2004; Watkinson et al., 2008, 2011; Ridd, 2009, 2012; Kanjanapayont et al., 2013)

The previous studies emphasize either ductile or brittle stages of the whole event. This study presents the deformation history of the Three Pagodas Fault based on the field work outcrop, petrography, and microstructure analysis. The whole deformation events are presented in this study. The results reveal the kinematic history of the Three Pagodas Fault.

2. Geological Background

The geology around the Three Pagodas Fault comprises a wide range of Paleozoic sedimentary rocks from Cambrian, Cambrian-Ordovician, Ordovician, Silurian-Devonian, Carboniferous-Permian, Permian, and Cenozoic sediment with the Triassic S-type granite in the northern part (Department of Mineral Resources, 2008). The metamorphic rock within the Three Pagoda shear zone or “Thabsila Gneiss” or “Thabsila metamorphic complex” has been subjected to high grade metamorphic rock (e.g., Nantasin et al., 2012; Kanjanapayont et al., 2018; Salypongse et al., 2020) of Precambrian (?) age (Department of Mineral Resources, 2008). The Thabsila metamorphic complex was subdivided into four units (Nantasin et al., 2012). Unit A comprises marble interbedded mica schist, fine-grained biotite gneiss and small outcrop of quartzite with the lowest pressure-temperature condition. Unit B is mylonite and mylonitic gneiss. Those rocks clearly show augen structure and a strongly deformed texture. Unit C is dominated by calc-silicate interbedded silicate bands. It presents a segregation layer between diopside layers and pure marble layers. Unit D has several compositions of gneiss. It mainly is composed of biotite gneiss, sillimanite gneiss, orthogneiss and mylonite.

The degree of metamorphism of high grade Thabsila metamorphic rock yielded medium amphibolite facies in unit A, whereas unit B, C, and D recorded the upper amphibolite facies. Another study subdivided the Thabsila Gneiss into 4 units: from oldest to youngest as Thabsila zone A, B, C, D (Salyapongse et al., 2020). Zone A is composed of migmatite, gneiss and cala-silicate. Zone B is mainly schist interbedded with fine grained paragneiss, quartz mica schist and calc-silicate to marble. Zone C shows quartzite, meta-limestone, phyllite to phyllitic schist and interbedded quartzite. Lastly, zone D is presented by fine grained slate, greenish grey color. Meta-sandstone and meta-limestone are exposed in the upper part of all Thabsila sequent.

3. Petrography

Based on the field mapping and petrography of this study, the metamorphic rocks in the Thabsila metamorphic complex are composed of high-grade and low-grade metamorphic rocks. The high-grade metamorphic rocks are divided into 6 units as migmatitic gneiss, augen gneiss, marble, schist, quartzite, and calc-silicate.

Migmatitic gneiss exposes at the center of complex zone. This unit shows discontinuous foliation and segregated melting of leucosome and mesosome. Mesosome layer is composed of medium to fine grained of feldspar, quartz, and tabular grain of biotite. The felsic layers of leucosome are extruded toward the fracture of mesosomes layers. The leucosome layers are mainly composed of quartz and plagioclase. These minerals show irregular, coarse to very coarse grained with grain boundaries migration.

Augen gneiss exposes as lens shape at the western and the eastern rims of the shear zone. It is characterized by augen-shaped megacrystals of K-feldspar with a strong gneissic foliation. This unit consists of medium to coarse grained and fine grained. The medium to coarse grains comprise K-feldspar, plagioclase, and quartz, whereas the finer grains are biotite, muscovite, and quartz. K-feldspar porphyloblases present myrmekite and twinning. Undulatory extinction generally presents in quartz. S-C and S-C' shear bands are a well-observed on an outcrop surface indicating sinistral shearing.

Marble exposes in the eastern and the western parts of the shear zone. The rock is characterized by fine to medium grained, white to gray color, granoblastic, and sugary textures. The mineral assemblage of the marble is mainly composed of calcite, graphite, plagioclase, muscovite, phlogopite, diopside, and quartz. Chlorite or iron oxide are accessory materials. Calcite displays fine to medium grained, subhedral, granoblastic, polygon and exhibits mossad textures. The twins slip plan is well-developed in the NW-striking, top-up-west direction as same as the maxima elongated orientation of their grains. Quartz normally shows undulatory extinction. S-C shear band and S-C' shear bands can be observed in this marble unit. All of the shear sense features clearly indicate sinistral movement.

Schist covered the western and the eastern parts by a variety in color and composition. Schistosity in NW-SE with NE-dipping is well-observed. The unit of schist can be subdivided into three types, including phyllitic schist, mica schist, and quartz schist. Phyllitic schist is characterized by fine grained, deep gray to back. Schistosity is well defined by fine grained mica that lies parallel in NW-SE. Quartz, muscovite, and biotite are the major mineral assemblages. Quartz shows very fine to fine in average < 0.1 mm with undulatory extinction. Chlorite and clay minerals are minor minerals.

Quartz-mica schist shows higher metamorphism than phyllitc schist. This rock has medium to coarse grained, bright brown to deep brown in and clearly displays schistosity. Quartz, muscovite, biotite, tremolite, and plagioclase are major mineral assemblage. Quartz strongly exhibits recrystallized deformation and oblique grain shape fabric. Most recrystallized grains reveal grain boundary migration and some sub-grain rotation. Muscovite and biotite strongly indicate the foliation plane in NW-SE. Muscovite is well developed more than biotite and altered to aluminosilicate mineral. Sillimanite and andalusite are common. Other minerals, such as garnet, zircon, and sericite, are accessory materials. Quartz schist has composition similar to mica schist, but quartz component is abundant. It displays medium to coarse grained, yellow to brown with a thickness less than 1 meter. A major mineral assemblage mainly composes of quartz, mica, hornblende, and garnet. Quartz shows an irregular grain, sheared deformation, undulose extinction, and recrystallization. Muscovite is fine grained with an average of 0.2 to 0.3 mm. Hornblende and garnet are accessory minerals. The oblique grain shape orientation and domino-type fragmented porphyroclasts in this schist unit indicate sinistral movement.

Quartzite exposes all over the shear zone, and is commonly interbedded with schist. The rock has fine to medium grained, colorless to yellow. It exhibits pencil structures on an outcrop. Quartz, a major mineral, shows medium grained with average of 0.3 to 0.5 mm, ribbon, and undulatory extinction.

Calc-silicate covers a wide area in the shear zone. It shows sugary granoblastic texture and compaction cleavage, segregating different component between green amphibole-diopside-rich layers and white or peach-colored feldspar-quartz-rich layers. Clinopyroxene, quartz, biotite, scapolite, plagioclase, and calcite are major mineral assemblages. Matrix of quartz and calcite forms as a small grain displaying undulatory extinction. In some area, calc-silicate exposed as folding and strong foliation. It is characterized by porphyroblast of plagioclase. Hornblende, pyroxene, epidote, chlorite, and muscovite are the matrix. S-C fabric in the calc-silicate clearly indicates sinistral sense of shear.

The low-grade metamorphic rocks can be found around the periptery of high-grade metamorphic unit. Outcrops of these rocks expose as an elongated lens in western side of the shear zone. This unit is composed of meta-pelitic rock and meta-carbonate rock.

Meta-pelitic rock is mainly composed of slate interbedded with phyllite. Quart, muscovite, and biotite indicates greenschist facies. The rock consists of quartz, biotite, chiolite major mineral assemblages.

Meta-carbonate is characterized by dark blue to gray, fine grained, and layers of meta-carbonate rich and argillaceous-rich. Lenticular-shape shows in some area. The major mineral assemblage composes of microcrystalline calcite, quartz, clay minerals, and opaque minerals. The darker band mainly composes of silicate, muds, and opaque minerals.

4. Structural geology

4.1. Foliations and lineations

Foliations of the high-grade metamorphic rocks show NW-SE striking with variation of dipping in both east and west directions (Fig. 2). In low-grade metamorphic unit, the NW-SE foliations orientate conformably to the high-grade metamorphic unit. Lineations in the high-grade metamorphic rock are exclusively recorded clearer than the low-grade metamorphic rock. They were defined by stretching grains of various minerals. The stretching lineations are clearly presented on the foliation plane of schist, quartzite, and augen gneiss. They generally orientate in NW-SE with sub-horizontal plunge.

4.2. Faults

The major faults in the area are characterized by oblique strike-slip faults. The strike of the fault planes shows a steeply dipping. These faults have an average orientation in NW-SE with high angle more than 70^{o} to 80^{o} to the west. The major oblique fault system regionally presents a dextral strike-slip with normal movement. The slickensides are dominantly orientated in NW-SE with sub-horizontal plunging to the NW. The fault breccia, which is mostly composed of fine to coarse grained, poorly sorted, and irregular shape, can be found along the fault planes.

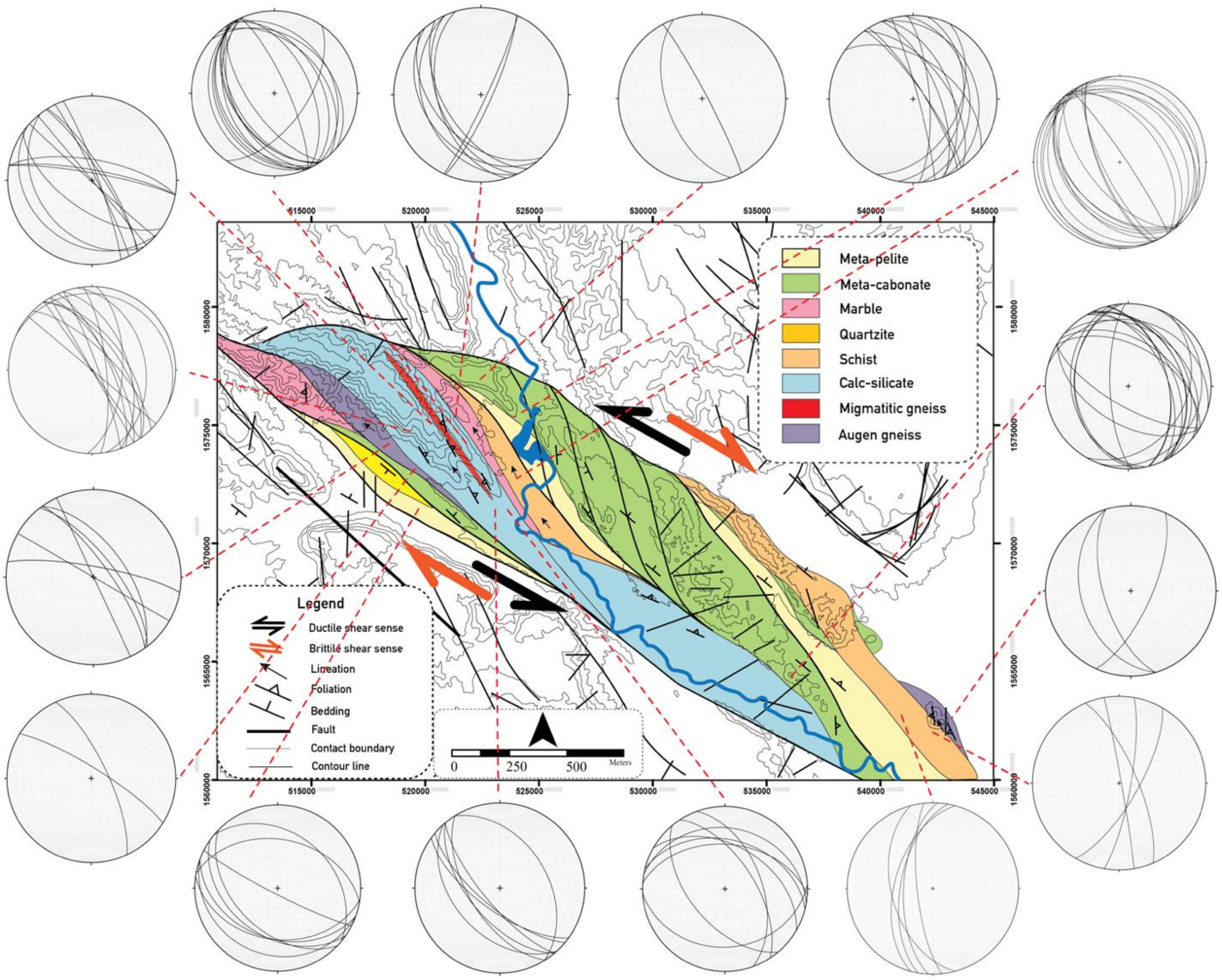

Figure 2 The foliations of the metamorphic rocks in the Three Pagodas Fault.

5. Discussions

5.1. Deformation history

Based on its kinematic evidence, the major deformation history of the Three Pagodas Fault is divided into D_1 and D_2. The D_1 can subdivided into D_{1a} and D_{1b} from the detailed structures.

5.1.1. D_{1a}

Within the Three Pagodas Fault, the metamorphic rock dominantly occurs as elongated lens shape that lies parallel in NW-SE direction. The result of mineral assemblages under polarizing microscope, the Thabsila metamorphic complex can be subdivided into two groups, one is greenschist metamorphic condition, and another is amphibolite metamorphic condition (Fig. 3). The greenschist facies was indicated by chlorite, biotite, muscovite, and quartz in the meta-pelitic rock. The amphibolite facies was represented by sillimanite, garnet, biotite, muscovite in schist, plagioclase, hornblende, pyroxene, diopside in calc-silicate rock, and quartz ribbon in quartzite. The greenschist metamorphic condition usually occurs around the peripheral of the metamorphic zone whereas the amphibolite metamorphic condition exposes at the center of the fault. The foliations have, generally, orientation in NNW-SSE striking, with a gentle dipping toward both west and east directions. On stereographic projection, they strike between 280° and 320° with dips between 80° and 60°. The foliations in high-grade metamorphic rocks show similar orientation to the low-grade metamorphic rocks, but their foliation planes have a small difference in the striking axis and average dip angles.

Microstructures in the Thabsila metamorphic complex clearly indicates sinistral movement. In low-grade metamorphic rocks, it exhibits kink bands of fine mica in meta-pelitic mylonite asymmetric folds of microcrystalline layers in meta-carbonate rocks. Sinistral microstructure features under microscopes of the high-grade metamorphic rocks are composed of elongated shape and oblique foliation, sigmoid, strain shadow, σ-porphyroclasts, S-C and S-C' shear bands. These features are in accord to the Mae Ping shear zone (Ponmanee et al., 2016), Ranong and Khlong Marui shear zone (Watkinson et al., 2008; Kanjanapayont et al., 2012) and Klaeng fault zone (Kanjanapayont et al., 2013).

Figure 3 Outcrops and photomicrographs of the high-grade metamorphic rocks in the Three Pagodas Fault; outcrop of schist (A), quartz + muscovite + biotite (Bi) in schist (B), outcrop of calc-silicate (C), plagioclases, hornblende, diopside, pyroxene in calc-silicate (D), sinistral shear indicator in augen gneiss outcrop (E), and sinistral movement of plagioclases porphyroblast in an augen gneiss sample (F). Qt is quartz, Ms is muscovite, Bi is biotite, Pl is plagioclase, Hb is hornblende, Kfs is K-feldspar and Sr is sericite.

In term of geochronology, U-Pb zircon rim dating of the mylonitic gneiss groups within D_1 phase show peak metamorphism around 51 – 57 Ma (Nantasin et al., 2012). These ages are close to U-Pb calcite vein dating from meta-carbonate mylonite at ~ 48 Ma (Simpson et al., 2021). Both documented data strongly indicate the beginning of sinistral strike-slip, which possibly causes metamorphisms of low-grade with high-grade metamorphic rocks along the Thabsila metamorphic complex. This timing relates to the onset of collision event between Indian-Eurasian plates, approximately between 50 – 65 Ma (Klootwojk et al., 1992; Molnar and Tapponier, 1975; Searle et al., 1997).

The field observed geology, structure, microstructure, and previous geochronological age data in sinistral strike-slip phase can be related to the major ductile deformation in the region. High-grade and low-grade metamorphic rocks deformed by the sinistral strike-slip movement were possibly metamorphosed at the same time but different position. High-grade metamorphic rocks were possibly associated with the deep crustal metamorphism and mineralization in the Thabsila metamorphic complex because pressure and temperature for high-grade metamorphism and ductile deformation are higher than the upper level, while low-grade metamorphic rock should be produced by the shallower level. This is in accord with many studies (Charusiri et al., 1993; Dill et al., 2008; Searle and Morley, 2011; Crow and Zaw, 2011; Nantasin et al., 2012). Moreover, the metamorphism period was possibly initiated during Late Paleocene – early Eocene, similar to Mae Ping shear zone (Meffer et al., 2007, Palin et al., 2013, Osterle et al., 2019), Klaeng fault zone (Geard, 2008, Kanjanapayont et al., 2013), and Ranong and Khlong Marui shear zones (Watkinson et al., 2011). On the basis of this suggestion, the sinistral ductile structure within the complex zone should be interpreted as the early-sinistral ductile strike-slip phase with both low-grade metamorphic condition at upper level and high-grade metamorphic condition at lower level. This condition characterizes the $D1_a$ phase of deformation history.

5.1.2. D_{1b}

This stage was compiled from the geological mapping and pervious works in geochronology. The presence of deep crustal rock at the surface suggested the exhumation in this zone. All of the cooling age data both inside and outside of the Three Pagodas Fault (Banopas, 1981), including Ar-Ar biotite dating (Lacassin et al. 1997), Sb-Sr biotite dating (Nantasin et al., 2012) and U-Pb calcite dating (Simpson et al., 2021), indicated ages of 33-35 Ma for the uplift of high-grade metamorphic rock from lower level to upper level. This marked the end of sinistral shearing. The spaced timing between peak metamorphism ages and cooling ages, averages between 40 – 30 Ma, we assume that transpressional strike-slip may occur during exhumation of high-grade metamorphic rock. This exhumation of high-grade metamorphic rock possibly affected from compaction principal stress axis from the India-Eurasia collision in W-E direction (Morley, 2012, Rhodes et al., 2005). The kinematic vorticity number of 0.75 – 0.99 from fry's method (Kanjanapayont et al., 2018) and ~ 0.95 (Ponmanee et al., 2016) have been obtained simple-shear dominated within metamorphisms during sinistral ductile deformation. The kinematic of this deformation is interpreted as the transpesstional tectonic.

5.1.3. D_2

The D_2 deformation in this area is indicated by the NW- SE treading system (Fig. 4). It presents a major dextral strike-slip fault in the region. This slip system is similar to anomaly solution of aeromagnetic analysis (Tulyatid & Rangubpit, 2016). The major fault systematically dominated and controlled younger structure at the surface. This fault system is initially interpreted as the boundary axes of the Thabsila metamorphic complex. It develops as an extensional pull-apart basin (Rhodes et al., 2005) and may occur as the extensional duplex in E-W direction. The N-S-trending is a minor fault, which can be observed in local scale. In-situ of calcite veins in meta-carbonate mylonite eastern side of the shear boundary yield U-Pb ages of ~23.5 Ma, (Late Oligocene to Early Miocene) (Simpson et al., 2021), similar to apatite fiction track of 23 -19 Ma (Upton et al., 1997). It is related to the reactivation of other strike-slip zones in Thailand (Morley, 2002) and changed of maxima compaction principal strain during clockwise rotation from E-W axes to N-S axes and decreased in magnitude (Rhodes et al., 2005). Then this deformation stage occurs after sinistral strike-slip deformation and completely wipes out older structure. The dextral strike-slip fault should be interpreted as the D_2.

5.2. Tectonic implications

The kinematic sharing deformation of the Three Pagodas Fault is related to the kinematic deformation of the India-Eurasia collision during

Eocene – recent (Upton, 1999; Morley, 2002; Rhodes et al., 2005; Nantasin et al., 2012; Kanjanapayont et al., 2018). The increase in the obliquely of subduction of the Indian plate to the west of SE-Asia is still moving northward (Molnar and Tapponnier, 1975) and resulted in movement along the indentation of India into Asia (Tapponnier et al., 1982) that is associated with the development of the major strike-slip fault (Lacassin et al., 1998; Socquet & Pubellier 2005; Morley, 2007) and high-grade metamorphic rock in the Thailand and adjacent area (Nantasin et al., 2012; Palin et al., 2013; Geard, 2008; Kanjanapayont et al., 2013; Watkinson et al., 2013).

The early period of the collision event resulted in compressive stress in front of the continent of the Indian plate (Tapponnier et al., 1982). At that time around 40 – 50 Ma, the horizontal compressive stress in this region has an orientation in W-E axis (Huchon et al., 1994), Sunderland thickness continent was slowly slied and extruded clockwise about 15^o southeastward (Yuyan and Morinaga, 1999; Rhodes et al., 2005). The increasing stresses along the NW-trending possibly occurred sinistral strike-slip fault along Three Pagodas Fault together with metamorphism within this region both in the upper and the lower levels, which was related to deformation shearing phase of D_{1a}. As this rotation continues, assuming between 15^o – 45^o orientation of the horizontal compressive stress remained to W-E trending (Maranate and Vella, 1986; McCabe et al., 1988), but their stress slowly changed southeastward from W-E axes to N-S axis. The changes would be interpreted as the exhumation and cooling down of deep metamorphic rock with transpressional tectonics and possibly related with exhumation the Thabsila high-grade metamorphic complex along the Three Pagodas Fault. This deformation was associated with the shearing phase of D_{1b}. As this rotation was completed, the orientation of horizontal compressive stress changed more than 45^o and the strike-slip fault removed their sense of movement from sinistral strike-slip to dextral strike-slip, leading to the development of pull-apart basin. These phenomena were interpreted to be deformation shearing phase of D_2.

The Three Pagodas strike-slip Fault deformed by the rotation stress pattern during Cenozoic is possibly linked with the Mae Ping shear zone on the northern edge (Morley, 2002), and the Ranong and Khlong Marui fault zones in the southern Thailand (Watkinson et al., 2013). Metamorphic period of those zone similar history to the Three Pagodas Fault between 40 – 50 Ma (Upton, 1999; Osterle et al., 2019; Meffre et al., 2007; Palin et al., 2013; Geard, 2008; Watkinson et al., 2011) is associated with metamorphism period of late Paleocene to middle Eocene, which was related to early collision between Indian – Eurasia Plates (Klootwojk et al., 1992; Molnar and Tapponnier, 1975; Searle et al., 1997). Similar to the cooling metamorphic ages, it is proposed that the uplift tectonics and exhumation of deep crustal metamorphic units of 30 – 35 Ma (Bignetl, 1972; Pitakpaivan, 1972; Banopas, 1981; Charusiri, 1989; Tulyatid, 1991; Ahrendt et al., 1993; Lacassin et al., 1997; Micckein, 1997; Kanjanapajont et al., 2013; Nachtergele et al., 2020) are related to the reactivation slip system in Thailand. Lastly, inversion period of this strike-slip zone has accommodated a large anastomosing pattern everywhere at upper level.

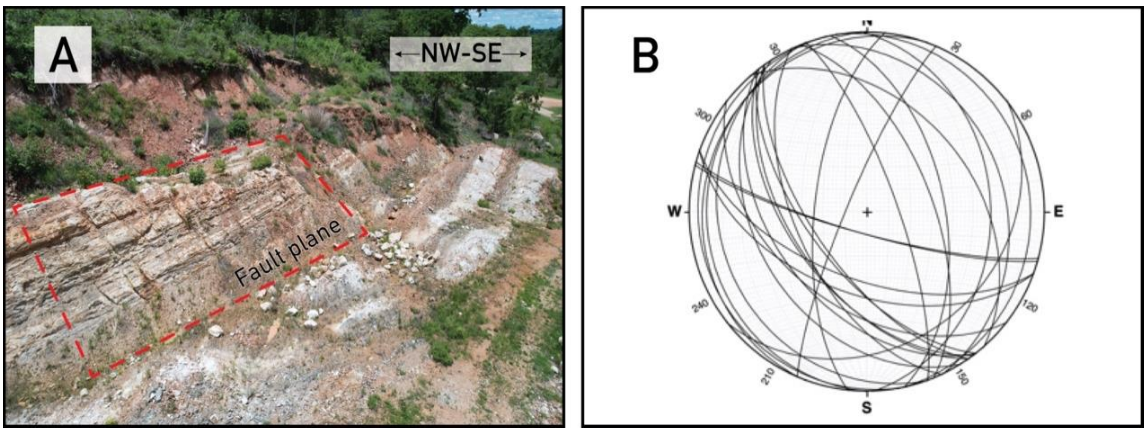

Figure 4 The brittle deformation of the last deformation in the Three Pagodas Fault.

6. Conclusions

The Three Pagodas Fault consists of a group of high-grade and low-glade metamorphic rocks. The high-grade metamorphic condition is amphibolite facies, and low-grade metamorphic condition is greenschist facies. The amphibolite facies unit is composed of migmatitic gneiss, augen gneiss, marble, schist, quartzite, and calc-silicate. The greenschist facies unit is mainly composed of meta-pelitic and meta-carbonate rocks.

The deformation history of the Three Pagodas Fault can subdivided into two deformation phases (Fig. 5) as follow;

D_{1a} is sinistral ductile strike-slip strain with low metamorphism grade at the upper level and high metamorphic grade at the lower level.

D_{1b} is sinistral ductile strike-slip with transpressional tectonics, which is related to the exhumation of lenses of high-grade metamorphic rock to the upper surface.

D_2 is dextral brittle strike-slip movement.

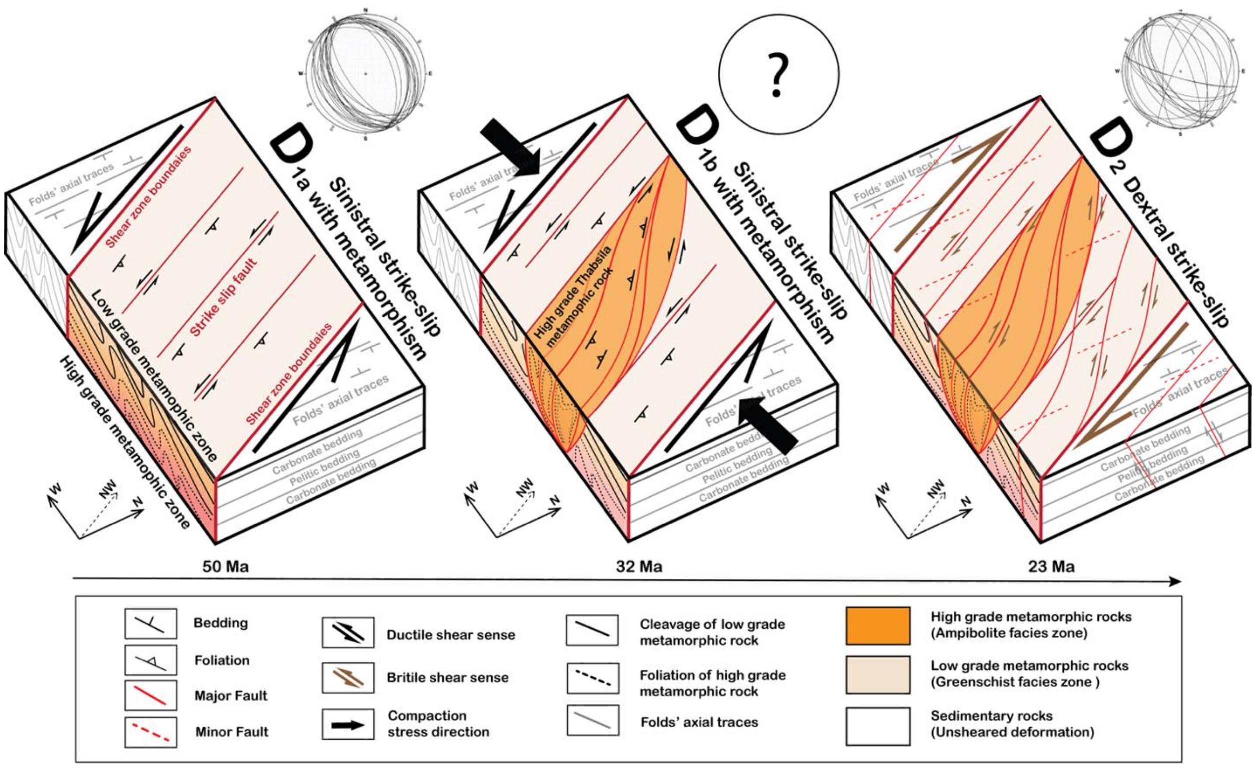

Figure 5 The two stages of the deformation history of the Three Pagodas Fault showing ductile sinistral shearing with metamorphism, transpression, and brittle dextral movement.

Acknowledgements

The research was funded by the Ratchadaphiseksomphot Endowment Fund, Chulalongkorn University. SK would like to acknowledge the development and promotion of the science and technology talented project (DPSD) through the Institute for the Promotion of teaching Science and Technology (IPST). We thank the Department of Geology, Chulalongkorn University, Thailand for the facilities to enable this research. Thanks are extended to the editor and anonymous reviewers for improving the manuscript.

References

AHRENDT, H., CHONGLAKMANI, C., HANSEN, B. & HELMCKE, D. 1993. Geochronological cross section through northern Thailand. Journal of Southeast Asian Earth Sciences, 8**,** 207-217.

BUNOPAS, S. 1976. Stratigraphic succession in Thailand. A preliminary summary. Journal of Geological Society of Thailand, 2**,** 37-58.

BUNOPAS, S. 1981. Paleogeographic History of Western Thailand and Adjacent Parts of Southeast Asia: A Plate Tectonics Interpretation, Geological Survey Paper No. 5. Department of Mineral Resources of Thailand, Bangkok, 810.

CHARUSIRI, P., CLARK, A. H., FARRAR, E., ARCHIBALD, D. & CHARUSIRI, B. 1993. Granite belts in Thailand: evidence from the 40Ar/39Ar geochronological and geological syntheses. Journal of Southeast Asian Earth Sciences, 8, 127-136.

CHARUSIRI, P., DAORERK, V., ARCHIBALD, D., HISADA, K. & AMPAIWAN, T. 2002. Geotectonic evolution of Thailand: A new synthesis. Journal of the Geological Society of Thailand, 1, 1-20.

CHUNG, S.-L., CHU, M.-F., ZHANG, Y., XIE, Y., LO, C.-H., LEE, T.-Y., LAN, C.-Y., LI, X., ZHANG, Q. & WANG, Y. 2005. Tibetan tectonic evolution inferred from spatial and temporal variations in post-collisional magmatism. Earth-Science Reviews, 68, 173-196.

CHUNG, S.-L., LEE, T.-Y., LO, C.-H., WANG, P.-L., CHEN, C.-Y., YEM, N. T., HOA, T. T. & GENYAO, W. 1997. Intraplate extension prior to continental extrusion along the Ailao Shan-Red River shear zone. Geology, 25, 311-314.

CHUNG, S.-L., LO, C.-H., LEE, T.-Y., ZHANG, Y., XIE, Y., LI, X., WANG, K.-L. & WANG, P.-L. 1998. Diachronous uplift of the Tibetan Plateau starting 40 Myr ago. Nature, 394, 769-773.

CROW, M. & ZAW, K. 2011. Metalliferous minerals.

DEPARTMENT OF MINERAL RESOURCES, 2008. Geological Map of Thailand, scale 1:50,000.

DILL, H., MELCHER, F. & BOTZ, R. 2008. Meso- to epithermal W-bearing Sb vein-type deposits in calcareous rocks in western Thailand; with special reference to their metallogenetic position in SE Asia. Ore Geology Reviews, 34, 242-262.

GEARD, A. 2008. Geology of the Klaeng Region (southeast Thailand): lithology, structure, and geochronology. BSc, Hons Thesis, University of Tasmania.

HUCHON, P., LE PICHON, X. & RANGIN, C. 1994. Indochina Peninsula and the collision of India and Eurasia. Geology, 22.

KANJANAPAYONT, P. 2015. Strike-slip ductile shear zones in Thailand.

KANJANAPAYONT, P., KIEDUPPATUM, P., KLÖTZLI, U., KLÖTZLI, E. & CHARUSIRI, P. 2013. Deformation history and U-Pb zircon geochronology of the high-grade metamorphic rocks within the Klaeng fault zone, eastern Thailand. Journal of Asian Earth Sciences, 77, 224-233.

KANJANAPAYONT, P., PONMANEE, P., GRASEMANN, B., KLÖTZLI, U. & NANTASIN, P. 2018. Quantitative finite strain analysis of the quartz mylonites within the Three Pagodas shear zone, western Thailand. Austrian Journal of Earth Sciences, 111, 171-179.

KLOOTWIJK, C. T., GEE, J. S., PEIRCE, J. W., SMITH, G. M. & MCFADDEN, P. L. 1992. An early India-Asia contact: paleomagnetic constraints from Ninetyeast ridge, ODP Leg 121. Geology, 20, 395-398.

LACASSIN, R., MALUSKI, H., LELOUP, P., HERVÉ, TAPPONNIER, P., HINTHONG, C., SIIRIBHAKDI, K., CHUAVIROJ, S. & CHAROENRAVAT, A. 1997. Tertiary diachronic extrusion and deformation of western Indochina: Structural and 40Ar/39Ar evidence from NW Thailand. Journal of Geophysical Research: Solid Earth, 102, 13 - 23.

LELOUP, P. H., LACASSIN, R., TAPPONNIER, P., SCHÄRER, U., ZHONG, D., LIU, X., ZHANG, L., JI, S. & TRINH, P. T. 1995. The Ailao Shan-Red River shear zone (Yunnan, China), Tertiary transform boundary of Indochina. Tectonophysics, 251, 3-84.

LIN, T.-H., CHUNG, S.-L., CHIU, H.-Y., WU, F.-Y., YEH, M.-W., SEARLE, M. P. & IIZUKA, Y. 2012. Zircon U–Pb and Hf isotope constraints from the Ailao Shan–Red River shear zone on the tectonic and crustal evolution of southwestern China. Chemical Geology, 291**,** 23-37.

MARANATE, S. & VELLA, P. 1986. Paleomagnetism of the Khorat Group, Mesozoic, Northeast Thailand. Journal of Southeast Asian Earth Sciences, 1**,** 23-31.

MCCABE, R., CELAYA, M., COLE, J., HAN, H. C., OHNSTAD, T., PAIJITPRAPAPON, V. & THITIPAWARN, V. 1988. Extension tectonics: The Neogene opening of the north–south trending basins of central Thailand. Journal of Geophysical Research: Solid Earth, 93**,** 11899-11910.

MOLNAR, P. & TAPPONNIER, P. 1975. Cenozoic Tectonics of Asia: Effects of a Continental Collision: Features of recent continental tectonics in Asia can be interpreted as results of the India-Eurasia collision. Science, 189**,** 419-26.

MORLEY, C. K. 2002. A tectonic model for the Tertiary evolution of strike–slip faults and rift basins in SE Asia. Tectonophysics, 347**,** 189-215.

MORLEY, C. K., CHARUSIRI, P. & WATKINSON, I. M. 2011. Structural geology of Thailand during the Cenozoic. In: RIDD, M. F., BARBER, A. J. & CROW, M. J. (eds.) The Geology of Thailand. Geological Society of London.

MORLEY, C. K., SMITH, M., CARTER, A., CHARUSIRI, P. & CHANTRAPRASERT, S. 2007. Evolution of deformation styles at a major restraining bend, constraints from cooling histories, Mae Ping fault zone, western Thailand. Geological Society, London, Special Publications, 290**,** 325-349.

NACHTERGAELE, S., GLORIE, S., MORLEY, C., CHARUSIRI, P., KANJANAPAYONT, P., VERMEESCH, P., CARTER, A., VAN RANST, G. & DE GRAVE, J. 2020. Cenozoic tectonic evolution of southeastern Thailand derived from low temperature thermochronology. Journal of the Geological Society, 177**,** 395-411.

NANTASIN, P., HAUZENBERGER, C., LIU, X., KRENN, K., DONG, Y., THÖNI, M. & WATHANAKUL, P. 2012. Occurrence of the high grade Thabsila metamorphic complex within the low grade Three Pagodas shear zone, Kanchanaburi Province, western Thailand: Petrology and geochronology. Journal of Asian Earth Sciences, 60**,** 68-87.

ÖSTERLE, J. E., KLÖTZLI, U., STOCKLI, D. F., PALZER-KHOMENKO, M. & KANJANAPAYONT, P. 2019. New age constraints on the Lan Sang gneiss complex, Thailand, and the timing of activity of the Mae Ping shear zone from in-situ and depth-profile zircon and monazite U-Th-Pb geochronology. Journal of Asian Earth Sciences, 181**,** 103886.

PALIN, R. M., SEARLE, M. P., MORLEY, C. K., CHARUSIRI, P., HORSTWOOD, M. S. A. & ROBERTS, N. M. W. 2013. Timing of metamorphism of the Lansang gneiss and implications for left-lateral motion along the Mae Ping (Wang Chao) strike-slip fault, Thailand. Journal of Asian Earth Sciences, 76**,** 120-136.

PONMANEE, P., KANJANAPAYONT, P., GRASEMANN, B., KLÖTZLI, U. & CHOOWONG, M. 2016. Quantitative finite strain analysis of high-grade metamorphic rocks within the Mae Ping shear zone, western Thailand. Austrian Journal of Earth Sciences, 109.

RHODES, B., CHARUSIRI, P., KOSUWAN, S. & LUMJUAN, A. 2005. Tertiary Evolution of the Three Pagodas Fault, Western Thailand.

RICHTER, B. & FULLER, M. 1996. Palaeomagnetism of the Sibumasu and Indochina blocks: Implications for the extrusion tectonic model. Geological Society, London, Special Publications, 106**,** 203-224.

SALYAPONGSE, S., SANTADGARN, P., HONG, P., JATUPORNKONGCHAI, S., CHANDON, E. & PUTTHAPIBAN, P. 2020. Transition between the Thabsila metamorphic complex and the Lower Paleozoic formations and their sandstone provenance, Kanchanaburi, western Thailand.

SEARLE, M., PARRISH, R., HODGES, K., HURFORD, A., AYRES, M. & WHITEHOUSE, M. 1997. Shisha Pangma leucogranite, south Tibetan Himalaya: Field relations, geochemistry, age, origin, and emplacement. The Journal of Geology, 105**,** 295-318.

SIMPSON, A., GLORIE, S., MORLEY, C. K., ROBERTS, N. M. W., GILLESPIE, J. & LEE, J. K. 2021. In-situ calcite U-Pb geochronology of hydrothermal veins in Thailand: New constraints on Indosinian and Cenozoic deformation. Journal of Asian Earth Sciences, 206**,** 104649.

TAPPONNIER, P., PELTZER, G. & ARMIJO, R. 1986. On the mechanics of the collision between India and Asia. Geological Society, London, Special Publications, 19**,** 113 - 157.

TAPPONNIER, P., PELTZER, G., LE DAIN, A. Y., ARMIJO, R. & COBBOLD, P. 1982. Propagating extrusion tectonics in Asia: New insights from simple experiments with plasticine. Geology, 10**,** 611-616.

TULYATID, J. 1991. A $^{40}Ar/^{39}Ar$ geochronological study of deformed meta - granitoid rocks adjacent to the Hua Hin - Pran Buri fault system, Peninsular Thailand. Master of Science, Queen’s University.

TULYATID, D. & RANGUBPIT, W. 2016. Subsurface Structure of Kanchanaburi Area Interpreted from Aeromagnetic Data. CHIANG MAI JOURNAL OF SCIENCE, 43**,** 1316-1323.

UPTON, D. R. 2000. A Regional Fission Track Study of Thailand: Implications for Thermal History and Denudation, University of London.

WATKINSON, I., ELDERS, C., BATT, G., JOURDAN, F., HALL, R. & MCNAUGHTON, N. 2011. The timing of strike-slip shear along the Ranong and Khlong Marui faults, Thailand. Journal of Geophysical Research, 116.

WATKINSON, I., ELDERS, C. & HALL, R. 2008. The kinematic history of the Khlong Marui and Ranong Faults, southern Thailand. Journal of Structural Geology, 30**,** 1554-1571.